ELSEVIER

Chemical Engineering Journal 99 (2004) 153–160

Chemical Engineering Journal
www.elsevier.com/locate/cej

Simulation of a fixed bed adsorber packed with protonated cross-linked chitosan gel beads to remove nitrate from contaminated water

K. Jaafari [a], T. Ruiz [b,*], S. Elmaleh [b], J. Coma [b], K. Benkhouja [a]

[a] *Groupe de Magnétochimie, Céramiques et Membranes, Faculté des Sciences, Université Chouaïb Doukkali, El Jadida, Morocco*
[b] *Laboratoire de Génie des Procédés d'Elaboration de Bioproduits, UMR CIRAD 016, CC 05, Université Montpellier II,*
34095 Montpellier Cedex 5, France

Accepted 13 October 2003

Abstract

Nitrate, contained in surface or groundwater, can be removed by sorption on protonated cross-linked chitosan gel beads. The sorption capacity is large enough to meet the standard of drinkable water. The isothermal equilibrium curves are straight lines which were established for a contaminated groundwater. The sorption kinetics is not limited by pore diffusion and is well modelled by a phenomenological equation. The experimental partition coefficient and overall mass transfer coefficient were used for simulating a plug flow fixed bed adsorber. The trend of the breakthrough curve was not affected by sinusoidal variations of the superficial velocity, which shows that the design can be carried out considering a conventional step injection. The breakthrough curve is more sensitive to the packing length than to the column diameter.

Keywords: Nitrate; Cross-linked chitosan; Groundwater; Plug flow reactor

---

1. Introduction

Water resources of many countries are heavily polluted by nitrate [1]. Nitrate concentration in groundwater or surface freshwater reaches, in some places, more than 100 mg l^{-1}. The actual European standard, of less than 50 mg l^{-1} in drinkable water, could become more stringent (25 mg l^{-1}). The major concern is the blue-baby syndrome resulting from the conversion of haemoglobin into methaemoglobin, which cannot carry oxygen [2]. If more than half the haemoglobin is converted, death is likely. Moreover, the adverse effects on adults are not well documented.

Nitrate removal is hampered by its low reactivity. Two treatment techniques are currently used, biological denitrification and ion exchange. Biological denitrification [3] requires a carbonaceous substrate and a subsequent polishing treatment like filtration and disinfection. This technique, inefficient at a temperature of lower than 7 °C, is generally carried out for groundwater which is constantly at a temperature of around 12 °C. Treatment by an ion-exchange resin replaces nitrate by chloride [4]. The resin retains also some sulphate and hydrogen-carbonate, inducing significant changes in the water composition and an increase of the chloride concentration. Moreover, the disposal of the concentrated effluent, obtained after regeneration, should be cautiously considered. Of course electrodialysis or reverse osmosis could also remove nitrate but high costs actually hamper their development.

Chitosan is a natural product derived by desacetylation from the polysaccharide chitin. Chitin is found in the exo-skeletons of shrimp, crab and other shellfish. Thanks to its exceptional properties, chitin protects these animals in their natural environment and its applications are growing in a large variety of other fields, e.g. carrier for immobilised cells, artificial skin, membrane synthesis, etc. [5]. Chitosan gel beads proved to be a particularly interesting adsorbent in the field of industrial wastewater treatment for the removal of heavy metals [5]. An extensive bibliography of its applications in water and wastewater treatment has been carried out [5]. However, no reference was found about its capacity to remove nitrate but the presence of amino groups [6], particularly in cross-linked chitosan, could favour anion adsorption. It has recently been shown that cross-linked chitosan gel beads, previously protonated, significantly adsorbed nitrate [7]. If required, the sorption capacity is easily recovered by increasing the pH to 12. But, considering that chitosan is a soil conditioner able to prevent crop diseases [8], saturated chitosan could be used as a fertiliser that

---

* Corresponding author. Tel.: +33-4-67-14-46-17;
fax: +33-4-67-14-47-87.
E-mail address: truiz@univ-montp2.fr (T. Ruiz).

1385-8947/$ – see front matter © 2004 Elsevier B.V. All rights reserved.
doi:10.1016/j.cej.2003.10.008

Nomenclature

A	matrix
C	liquid phase solute concentration $[\mathrm{ML}^{-3}]$
C^*	liquid phase concentration in equilibrium with adsorbed solute $[\mathrm{ML}^{-3}]$
C_e	final or outlet liquid phase solute concentration $[\mathrm{ML}^{-3}]$
C_0	initial or inlet liquid phase solute concentration $[\mathrm{ML}^{-3}]$
f	dimensionless concentration in the solid phase
k	overall mass transfer coefficient $[\mathrm{T}^{-1}]$
K	kL/u_0
m	partition coefficient $[\mathrm{L}^3\,\mathrm{M}^{-1}]$
q	solid phase solute concentration
q_e	final solid phase solute concentration
r	removal rate $[\mathrm{ML}^{-3}\,\mathrm{T}^{-1}]$
S	vectorial sum
t	time [T]
u	superficial velocity $[\mathrm{LT}^{-1}]$
u_0	mean superficial velocity $[\mathrm{LT}^{-1}]$
U	u/u_0
x	dimensionless abscissa
z	abscissa [L]
Z	dimensionless time
Greek letters	
α	$1/m\chi$
β	$1/m\rho$
γ	dimensionless concentration in the liquid phase
ε	bed porosity
ρ	$((1-\varepsilon)/\varepsilon)\rho_S$ $[\mathrm{ML}^{-3}]$
ρ_S	gel density $[\mathrm{ML}^{-3}]$
χ	adsorbent concentration $[\mathrm{ML}^{-3}]$
ω	pulsation $[\mathrm{T}^{-1}]$
ϖ	$\omega u_0/L$

slowly liberates nitrate. This work establishes the equilibrium law for the solute in the liquid and solid phases and the adsorption kinetics in the case of contaminated groundwater. This information is then used to simulate and design, without adjusting any parameter, the operation of a fixed bed adsorber treating groundwater for a small community.

2. Experimental

Chitosan gel beads were made by means of the following procedure: chitosan powder, provided by France Chitine, was dissolved in an acetic acid solution of same concentration as the solid (3.5 mass%). The solution was then pumped through a hypodermic needle allowing drops to fall down into a tank containing a 2 M NaOH solution. Heterogeneous precipitation induced the formation of highly porous spherical gel beads, which settled at the bottom of the tank. Injecting air, at different flowrates, around the falling drop enabled varying the bead size. After 12 h, the beads were washed with distilled water in order to reach neutrality. Cross-linked gel beads were obtained after 24 h residence time in a glutaraldehyde solution (5 g g^{-1} dry chitosan) [9]. The beads were then cautiously washed with distilled water. The material (100 g l^{-1} beads) was protonated by 30 min gentle stirring in a HCl solution, the concentration of which conditioned the equilibrium pH of the sorption runs.

All the equilibrium and kinetics runs were carried out in 0.5 l batch reactors, mechanically stirred, at 80 rpm in current operation. Equilibrium was reached after 10–20 min. The nitrate solution was groundwater (20 mg l^{-1} nitrate concentration) from the Montpellier region, in France, to which sodium nitrate was added. All the runs were carried out at room temperature which was maintained at 20 °C. Nitrate concentration was determined by the spectrophotometric technique with 5% accuracy (spectrophotometer HACH DR 2000 and Nitraver reagent). pH was monitored with a WTW pH 95 pH-meter.

3. Results and discussion

3.1. Sorption equilibrium and kinetics

The equilibrium nitrate concentration q_e retained on the solid phase was calculated by a mass balance between the initial and the final states:

$$q_e = \frac{C_0 - C_e}{\chi} \tag{1}$$

where χ is the adsorbent concentration, C_0 and C_e being respectively the initial and equilibrium concentrations. In the studied range of nitrate concentrations, the equilibrium curves were straight lines (Fig. 1) whose slope, the partition coefficient, depended on pH which slightly increased, during the sorption step, of 0.1–0.3 pH unit [7]. Different values of final pH were obtained by using different volumes of hydrochloric acid in the protonation step. The partition coefficient varies against pH according to a bell-shaped curve (Fig. 2). The sorption is maximum at pH between 3 and 5 and low beyond 6, a value close to the chitosan 6.2 pK_A [6]. At pH lower than 2, the sorption is very weak as a probable result of the breakage of bonds between functional amino groups and glutaraldehyde.

Some chemical considerations explain the shape of the partition coefficient curve. Reticulated chitosan gel is an imine whose protonation can be described by [10]

$$\mathrm{RCH{=}NR'} + \mathrm{H^+} \rightleftarrows \mathrm{RCH{=}N^+HR'} \tag{2}$$

where R and R′ are carbonaceous cycles. The acidity of the charged RCH=N$^+$HR′ group was put into evidence by potentiometric titration [7]. The titration curve of the non-cross-linked gel has two inflexion points corresponding

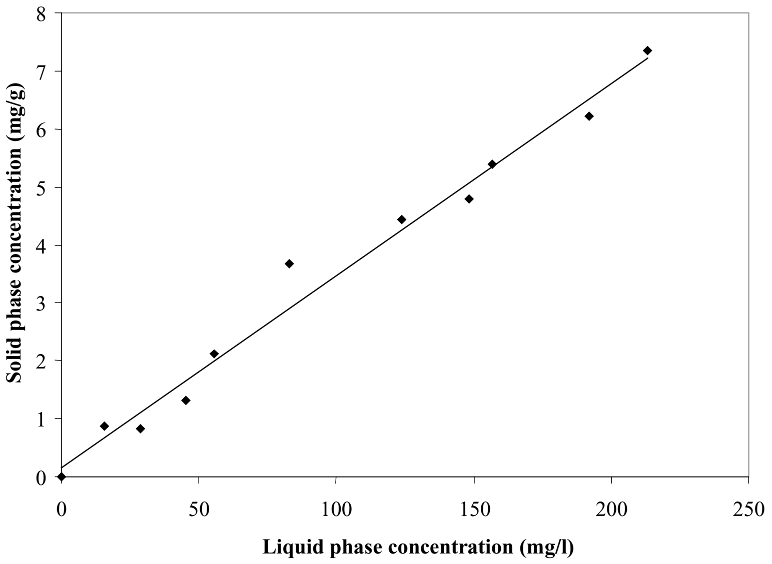

Fig. 1. Equilibrium curve (groundwater, 4.5 mm gel beads, final pH 4).

to the mixture of a strong acid (HCl) and a weak acid NH_3^+ that is a protonated amine [7,11]. On the other hand, the titration curve of cross-linked chitosan has only one transition point exactly like HCl [7]. The $RCH{=}N^+HR'$ group reacts with water in two steps [8]; first with OH^-

$$RCH{=}N^+HR' + OH^- \rightleftarrows RCH(OH){-}NHR' \qquad (3)$$

Then with H^+:

$$RCH(OH){-}NHR' + H^+ \rightleftarrows RCH(OH){-}NH_2{}^+R' \qquad (4)$$

$RCH(OH){-}NH_2{}^+R'$ is a secondary ammonium group, particularly reactive and able to retain anions [9]:

$$RCH(OH){-}NH_2{}^+R' + NO_3{}^- \rightleftarrows RC(OH)H{-}NH_2{}^+R', NO_3{}^- \qquad (5)$$

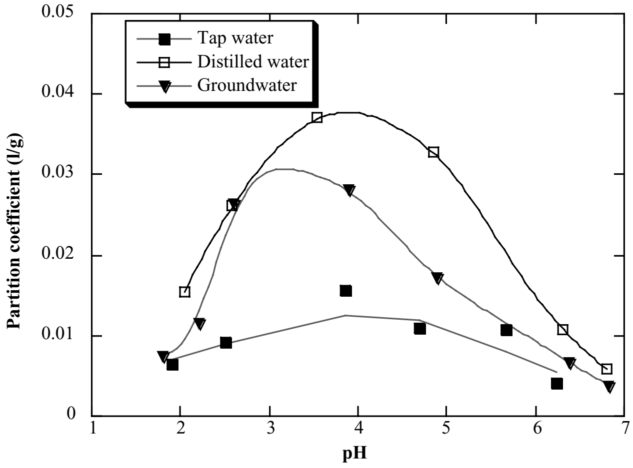

Fig. 2. Partition coefficient against pH for different types of water (4.5 mm gel beads).

Both steps (3) and (4) are required for nitrate removal by Eq. (5) and an intermediate convenient pH value will maximise the partition coefficient. However, the nitrate removal at pH of around 7 is significant enough to consider groundwater treatment.

Moreover, the final equilibrium depends on the total bead volume, and not on its external surface area. The sorbed concentration at equilibrium was indeed found to be identical with same mass, and therefore, the packing porosity being unchanged, same volume, of 1.5 and 4.5 mm diameter gel beads (Fig. 3). The specific area of a spherical particle being inversely proportional to its diameter, the external surface area per unit volume offered by a sample of 1.5 mm beads is nine times larger than the external area of a 4.5 mm sample of same volume. Examples of such reactions are frequent with biofilm coated particles or gels [12].

The equilibrium was rapidly reached in a batch reactor, while the transient concentration and therefore, the kinetics were close for different bead sizes (Fig. 4). In fact, the rate was slightly slower with 1.45 than with 4.5 mm beads, which is quite unexpected since an internal diffusion resistance would increase with the bead size. The impact of size on the kinetics will be quantified later using a rate equation. Moreover, no slow nitrate depletion was observed that could be related to an internal diffusion process. In all the runs, the reaction was completed after 10–20 min depending on the pH [7].

On the other hand, a low turbulence level is sufficient to eliminate a fraction of the liquid–solid resistance, i.e. film diffusion around the particle, since the kinetics was found independent of the stirring velocity at 40 rpm; film diffusion is possibly eliminated between 10 and 40 rpm (Fig. 5), i.e. at low energy dissipation. The residual resistance, which was measured as shown later, corresponds probably to a film

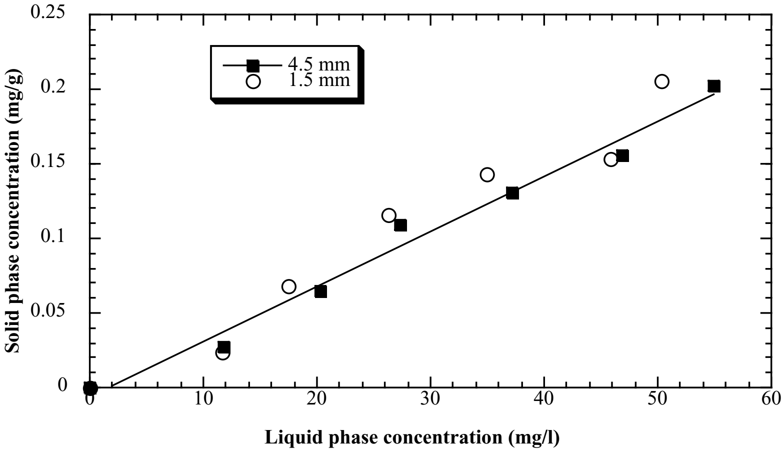

Fig. 3. Equilibrium curve for 1.5 and 4.5 mm gel beads (distilled water, pH = 6.2).

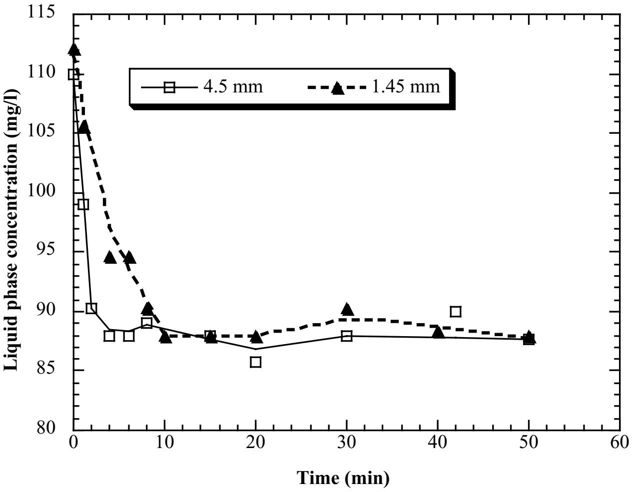

Fig. 4. Liquid phase concentration against time for two different bead sizes (groundwater, final pH 6).

diffusion resistance located inside the particle and not on its external surface. The difference with conventional situations, where catalysts are involved, comes from the high porosity evaluated at 0.92 [13].

The removal rate r can be expressed by the following widely used phenomenological equation [14]:

$$r = -k(C - C^*) \tag{6}$$

where k is an overall transfer coefficient and C^* the nitrate concentration in the liquid phase which would be in equilibrium with the sorbed concentration q:

$$q = mC^* \tag{7}$$

m being the partition coefficient. Besides, the transient state mass balance, in a batch reactor, is

$$\mathrm{d}q = -\frac{1}{\chi}\mathrm{d}C \tag{8}$$

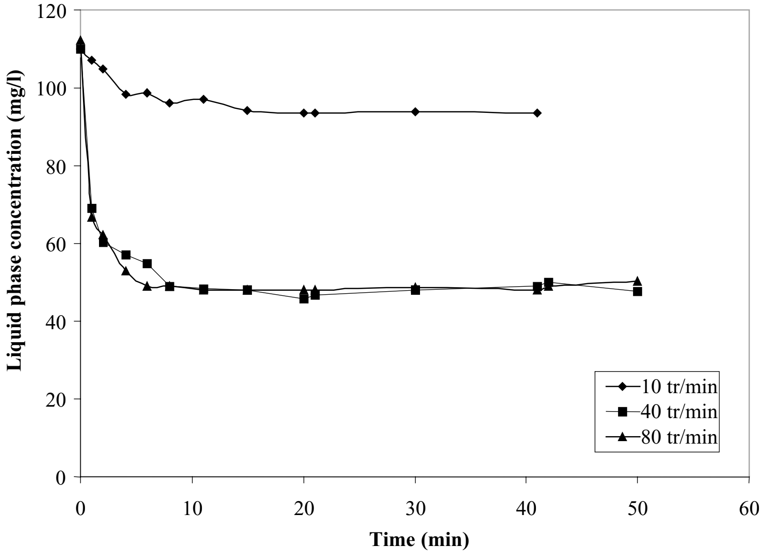

Fig. 5. Liquid phase concentration against time for different stirring speeds (groundwater, 4.5 mm gel beads, final pH 6).

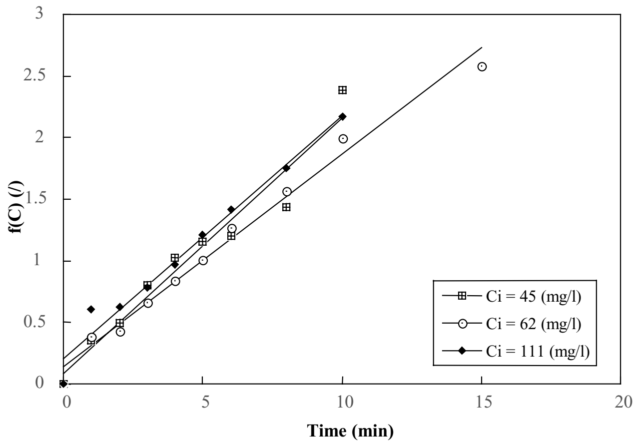

Fig. 6. *f*(*C*) against time for different initial concentrations (groundwater, sorption at pH 6.8).

By combining these equations and integrating, the transient concentration is obtained

$$\frac{C}{C_0} = \frac{1}{1+\alpha}(\alpha + e^{-k(1+\alpha)t}) \quad \alpha = \frac{1}{m\chi} \tag{9}$$

The model accuracy can be evaluated using the following equivalent equation, which should give a straight-line plot

$$f(C) = -\frac{1}{1+\alpha}\ln\left[(1+\alpha)\frac{C}{C_0} - \alpha\right] = kt \tag{10}$$

The plot of *f*(*C*) against time is indeed a straight line, which does not depend on the initial concentration (Fig. 6). The k value depended on pH, e.g. 0.4 min^{-1} at pH 3 and 0.04 min^{-1} at pH 7.3. With the data of Fig. 4, the transfer coefficient is 0.29 min^{-1} when using 1.45 mm beads and 0.33 min^{-1} with 4.5 mm beads. The 12% difference, which is the order of magnitude of the experimental accuracy, will be neglected.

3.2. Simulation of a plug flow reactor

In a plug flow packed column, the mass balances in the liquid and solid phases are respectively:

$$\frac{\partial C}{\partial t} + u\frac{\partial C}{\partial z} + k(C - C^*) = 0 \tag{11}$$

and

$$\frac{\partial q}{\partial t} = \frac{k}{\rho}(C - C^*) \tag{12}$$

where z is the abscissa in the packed column and u is the superficial velocity. The variable ρ is given by

$$\rho = \frac{1-\varepsilon}{\varepsilon}\rho_S \tag{13}$$

where ρ_S is the gel density and ε is the porosity of the bed. The initial conditions are

$$C(z, 0) = 0, \qquad q(z, 0) = 0 \tag{14}$$

The limit conditions, for an injection at constant inlet concentration C_0, are

$$C(0, t) = C_0, \qquad \left(\frac{\partial C}{\partial z}\right)_{z\to+\infty} = 0 \tag{15}$$

Two situations were simulated. The first one corresponds to the conventional step injection where the superficial velocity is constant (u_0). However, in current operation of such an exchanger, the superficial velocity could be transient. In most cases, the flowrate is periodic. The second situation corresponds then to a transient superficial velocity u according to a sinusoidal law

$$u = u_0\left[1 + \sin\left(\omega t - \frac{\pi}{2}\right)\right] \tag{16}$$

where u_0 is the mean value of the superficial velocity and ω is the pulsation.

Dimensionless variables were introduced:

- dimensionless abscissa $x = z/z_0$;
- dimensionless time $Z = u_0 t/L$, where L is the reactor length;
- dimensionless concentration in the liquid phase $\gamma = C/C_0$;
- dimensionless concentration in the solid phase $f = q/mC_0$.

Taking into account the equilibrium given by Eq. (7), the balance equations become

$$\frac{\partial \gamma}{\partial Z} + U\frac{\partial \gamma}{\partial x} + K(\gamma - f) = 0 \tag{17}$$

$$\frac{\partial f}{\partial Z} = \beta K(\gamma - \gamma^*) \tag{18}$$

with $K = kL/u_0$, U the u/u_0 ratio (1 in case of constant flowrate) and $\beta = 1/m\rho$

$$U = 1 + \sin\left(\varpi Z - \frac{\pi}{2}\right) \tag{19}$$

with $\varpi = (\omega u_0/L)$. The initial and boundary conditions are:

$$\gamma(x, 0) = 0, \qquad f(x, 0) = 0, \qquad \gamma(0, Z) = 1, \qquad \left(\frac{\partial \gamma}{\partial Z}\right)_{x\to+\infty} = 0$$

In constant flowrate operation, the model has only two parameters β and K that are determined from the batch run data. The mathematical problem is constituted by the two coupled partial derivative Equations (17) and (18). Their solution was obtained by a numerical method.

Eq. (17) was discretised by finite differences with an implicit time scheme and a space gradient taken at the left. Such a discretisation scheme has the advantage of being unconditionally stable. The linearisation consists in solving the equation by considering the variables γ and f at the preceding step. The calculation was carried out on a length larger than L in order to satisfy the boundary condition at the column outlet; then, only the values obtained inside the column were taken into account. The linearised problem can be stated under the following matricial form:

$$A(Z-\Delta Z)\gamma(Z) = S(Z-\Delta Z) \tag{20}$$

where $A(Z-\Delta Z)$ is a multidiagonal matrix, whose non-constant terms are actualised at each time step, and $S(Z-\Delta Z)$ is the vectorial sum of the concentration vector at $A(Z-\Delta Z)$ and the boundary conditions. The vector solution $\gamma(Z)$ was obtained, at each time step, by multiplying the second member by the inverse of the matrix $A(Z-\Delta Z)$. Eq. (18) was discretised by finite differences; the vector $q(x, Z)$ was determined immediately after $\gamma(Z)$. Its value was then introduced in the discretised Eq. (18). The numerical problem was programmed on Matlab® 4.2c. The problem was solved with the numerical values given in Table 1 (0.01 m spatial step and 60 s time step). All the equilibrium and kinetic parameters were determined with the batch reactor data. The mean flowrate was in conformity with the water demand of 5–10 people since such a process seems suitable for treating water of a small community at a domestic level.

Table 1
Numerical values for the simulation

Variable	Value
Inlet concentration, C_0 (mg/l)	100
Mean flowrate (l/h)	42
Flowrate period (h)	4 or 6
Mass-transfer coefficient, k (min^{-1})	0.21
Partition coefficient, m (l/g)	0.033
Gel bead density, ρ_S (kg/m^3)	1067
Bed porosity, ε	0.4

The response to a step injection, at constant superficial velocity, has the conventional sigmoid shape of a breakthrough

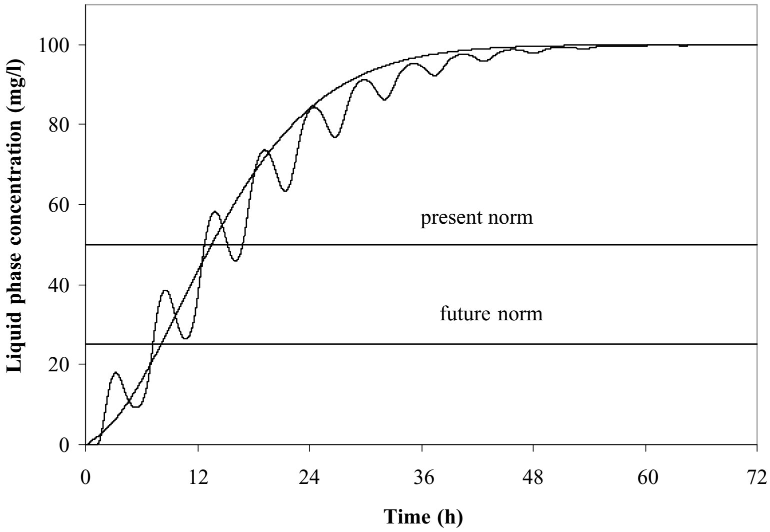

Fig. 7. Breakthrough curve through a packed column ($L = 1$ m, 0.15 m diameter, 4 h period).

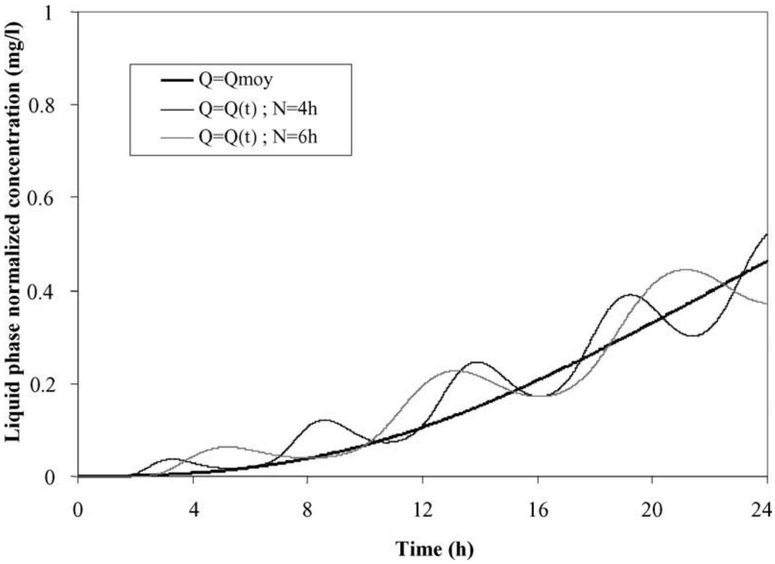

Fig. 8. Beginning of the breakthrough curve for two period values ($L = 1$ m, 0.2 m diameter).

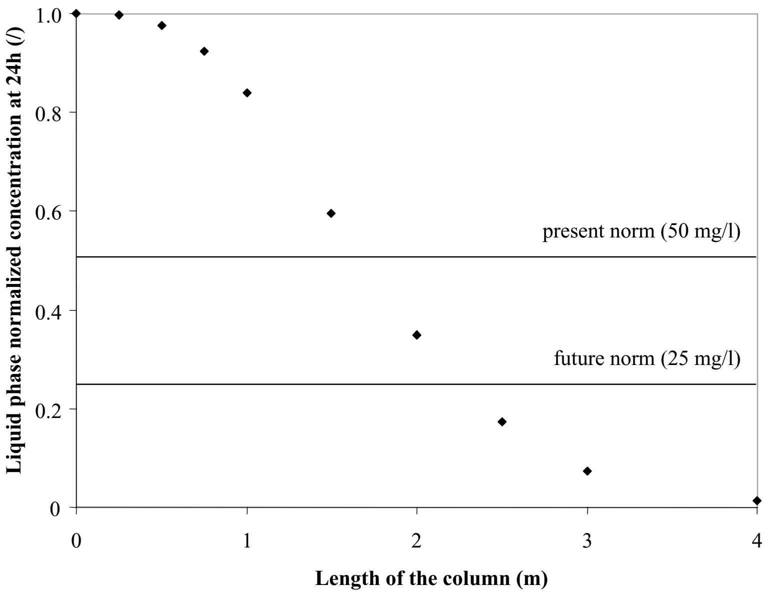

Fig. 9. Outlet concentration against packing length after 24 h operation (0.15 m diameter).

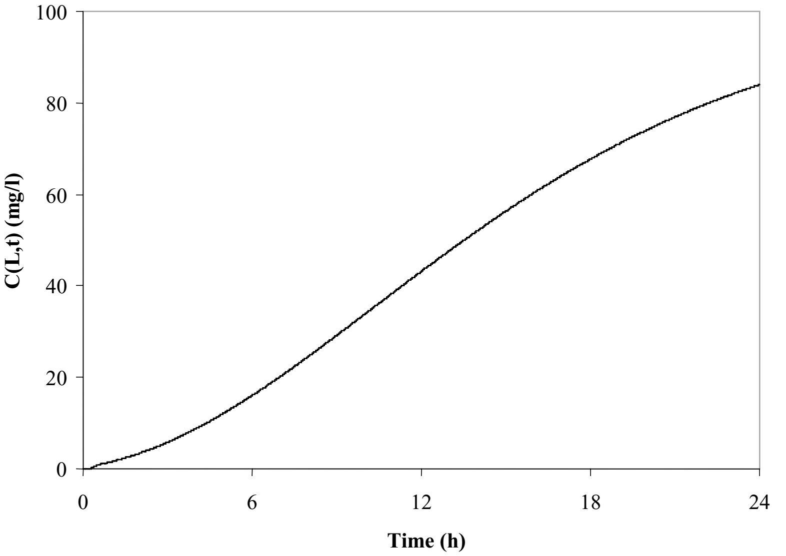

Fig. 10. Outlet concentration against diameter after 24 h operation (1 m length).

curve (Fig. 7). If the superficial velocity varies sinusoidally, the overall trend of the response is not affected (Fig. 7). The conclusion can be extended to any periodic superficial velocity by decomposition in Fourier series. This observation was confirmed by simulating at a smaller interval of time and for different pulsations (Fig. 8). A design, carried out for a steady velocity, could be therefore, easily extended to the case of a transient velocity.

The adsorber can be designed by calculating the outlet concentration after 24 h operation against the diameter or the length, this duration being acceptable for a small community. Fig. 9 shows, for a 0.15 m diameter column, that the unit should be packed on 1.5 m length if the actual standard of 50 mg l^{-1} is to be met. If the concentration should be less than 25 mg l^{-1}, the packing must be 2 m long. An analogous approach applies if the length is maintained constant and the diameter is to be calculated (Fig. 10). In both cases, a diameter of around 0.2 m is suitable. The outlet concentration is then more sensible to the length than to the diameter.

4. Conclusions

(1) Protonated cross-linked chitosan gel can significantly remove nitrate contained in contaminated water.
(2) Internal diffusion cannot be put into evidence.

(3) Liquid–solid mass resistance on the external surface is eliminated by slight turbulence.
(4) The main resistance corresponds to film diffusion inside the particle.
(5) The breakthrough curve of a plug flow adsorber is not significantly affected by transient superficial velocity and the design can be carried out with a conventional step injection.
(6) The efficiency of a plug flow adsorber is more sensitive to its length than to its diameter.
(7) If the simulation is accurate, daily water required for 5–10 people, consuming 300 l per people day, could be produced with an adsorber of 0.2 m diameter and 1.5 m length.
(8) Chitosan could be the basis of an alternative denitration process, which could find application at a domestic scale, the saturated particles being collected and used as fertiliser and soil conditioner. However, more work is required to evaluate the cost-effectiveness compared to more conventional processes.

References

[1] D. Laigla, J. Kugler, H. Kobus, L. Zilliox, Contamination des eaux souterraines par les nitrates, Recherche et application dans le cadre de la coopération franco-allemande, Inf. Eaux 1 (1990) 1–26.
[2] P.J. Golden, R. Weinstein, Treatment of high-risk refractory acquired with automated red blood cell exchange, J. Clin. Aphresis 13 (1) (1998) 28–31.
[3] Y. Richard, A. Leprince, L'azote dans le traitement des eaux potables-Les traitements biologiques, L'Eau 4 (1980) 167–181.
[4] A. Deguin, Incidence des résines échangeuses d'anions sur la qualité de l'eau traitée selon le procédé nitracycle, L'Eau 4 (1988) 213–234.
[5] C. Milot, Adsorption de Molybdate VI sur Billes de Gel de Chitosane. Application au Traitement d'Effluents, Doctorate Thesis, Université Montpellier II, 1998, p. 256.
[6] R.A.A. Muzzarelli, Chitin, Pergamon Press, Oxford, 1977, p. 356.
[7] K. Jaafari, S. Elmaleh, J. Coma, K. Benkhouja, Equilibrium and kinetics of nitrate removal by protonated cross-linked chitosan, Water SA 27 (2001) 1.
[8] A. El Ghaouth, J. Arul, J. Grenier, A. Asselin, Antifungal activity of chitosan on two postharvest pathogens of strawberry fruits, Phytopathology 82 (4) (1992) 398–402.
[9] H. Yoshida, A. Okamoto, H. Yamasaki, T. Kataoka, Fundamentals of Adsorption, Kodansha, Tokyo, 1993, p. 402.
[10] G.A.F. Roberts, K.E. Taylor, Chitosan gels-3: the formation of gels by reaction of chitosan with glutaraldehyde, Makromol. Chem. 190 (1989) 951–960.
[11] H. Yoshida, N. Kishimoto, T. Kataoka, Adsorption of strong acid on polyaminated highly porous chitosan: equilibria, Ind. Eng. Chem. Res. 33 (1994) 854–859.
[12] S. Elmaleh, Rule of thumb modelling of biofilm reactors, Water. Sci. Technol. 22 (1/2) (1990) 405–418.
[13] T. Mitani, N. Fukumuro, C. Yoshimoto, H. Ishi, Effects of counter ions (SO_4^{2-} and Cl^-) on the adsorption of copper and nickel ions by swollen chitosan beads, Agric. Biol. Chem. 55 (1991) 2419–2426.
[14] P. Le Goff, Energétique Industrielle, Technique et Documentation, Paris, 1979, p. 376.